



## Synchronous Control of Multi-Mover PMLSM Using Ring Coupling Control Strategy with Sliding Mode

---

Jinglong Zhong, Bao Song, Hu Li and Xiangdong Zhou

EasyChair preprints are intended for rapid dissemination of research results and are integrated with the rest of EasyChair.

March 31, 2023

# Synchronous Control of Multi-mover PMLSM Using Ring Coupling Control Strategy with Sliding Mode

Jinglong Zhong<sup>a</sup>, Bao Song<sup>a</sup>, Hu Li<sup>b</sup>, Xiangdong Zhou<sup>\*a</sup>

*a. School of Mechanical Science and Engineering, Huazhong University of Science and Technology*

*b. Guangdong Intelligent Robotics Institute, Dongguan, xdzhou2016@163.com*

**Abstract** - For the synchronous control of multi-mover permanent magnet linear synchronous motors (PMLSM) which is widely used in logistics equipment, a control method for the synchronization of multi-mover is developed by combining sliding mode control and ring coupling control strategy. Define the speed error of the two movers as the synchronization error, and introduce it into the control system of the previous mover, to improve the synchronization accuracy between the movers. Moreover, the stability of the control system is proved by the Lyapunov stable theory. The experimental results of the four-mover synchronous control system show that the proposed method can enhance the speed tracking and synchronization error of the platform effectively.

## INTRODUCTION

The control of single movers has been difficult to meet the application requirements in the fields of rail transit, computer numerical control machine tools, lithography machines, and robotics[1-5]. To obtain better product quality, reduce errors, and improve system security, it is of great significance to study a multi-mover synchronous control strategy[6-8].

The multi-movers synchronous system is a time-varying nonlinear system. The change in system parameters and the disturbance of load thrust will affect the synchronization of the system[9, 10]. In terms of control strategies, the current control systems are mainly divided into two categories: uncoupled control and coupled control. Among them, the uncoupled control methods include master-slave control, parallel control, and virtual-shaft control[11-14]. These uncoupled control methods have achieved several results and have been applied in some fields. However, since there is no coupling between the motors when one of the motors is disturbed, it is difficult for the other movers to adjust accordingly, resulting in the system synchronization being poor.

The idea of coupling control was first introduced into the synchronous control of dual motors and a coupling control strategy with compensation was proposed: cross-coupling control[15]. This control structure achieved a certain synchronization performance by compensating the actual error between the speed of two motors, but it is difficult to be extended to the control of more than two motors[16]. On this basis, an adjacent cross-coupling control strategy was proposed for exceeding three motors[17]. However, it has a poor dynamic characteristic as the synchronous error generated by adjacent motors, and the certain lag produced by the

transmission. Furthermore, the deviation coupling control strategy was proposed to solve the control delay problem of cross-coupled control by compensating the deviation value of one motor from other motors as a synchronization error[18]. But the control system becomes very complex as the number of motors increases. Compared with cross-coupling control and deviation-coupling control, ring-coupling control[19, 20] has stronger scalability and a simpler control structure.

However, the control effect of the ring coupling control strategy is easily affected by system disturbances. Sliding mode control has the property of being insensitive to parameters. To reduce the influence of system disturbance on synchronous control accuracy, a sliding mode ring-coupling control strategy is proposed for the multi-mover PMLSM in this paper. In this method, the sliding mode control is introduced into the ring-coupling structure to improve the precision of the synchronous control simultaneously. The structure of this article is organized as follows: Section A introduces the mathematical model of the PMLSM. In Section B, the ring-coupling synchronization structure is designed. And the speed tracking and synchronization controller based on sliding mode is designed in Section C. The control effect compared with the traditional cross-coupling control method by the experiments is given in Section 5. Finally, Section E sets out the conclusion.

### A. PMLSM Mathematical Model

The mathematical model of PMLSM is described as follows:

$$\begin{cases} u_d = R_s i_d + L_d \cdot di_d/dt - \omega_e L_q i_q \\ u_q = R_s i_q + L_q \cdot di_q/dt + \omega_e L_d i_d + \omega_e \psi_f \end{cases} \quad (1)$$

Among them,  $u_d/u_q$  and  $i_d/i_q$  are  $d/q$  axis stator voltage and current, respectively.  $R_s$  is the winding resistance, and  $L_d/L_q$  is the  $d/q$  axis stator inductance, respectively.  $\psi_f$  is the permanent magnetic flux linkage.  $\omega_e = \pi v/\tau$  is the electrical angular speed, where  $v$  is the linear speed of the mover and  $\tau$  is the pole distance.

The electromagnetic power equation of PMLSM is:

$$F_e = 3\pi/2\tau \cdot [\psi_f i_q + (L_d - L_q) i_d i_q] \quad (2)$$

The motor dynamic equation can be obtained as:

$$M\dot{v}(t) + Bv(t) = F_e - F_l \quad (3)$$

Among them,  $F_e$  is the thrust of the motor.  $F_l$  is the thrust of the load.  $M$  is the mass of the mover.  $B$  is the viscous friction coefficient.

In the vector control mode  $i_d = 0$ ,  $L_d = L_q = L$  is approximately considered. And the following equation can be obtained.

$$\begin{cases} F_e = 3\pi/2\tau \cdot \psi_f i_q = K_f i_q \\ u_q = R_s i_q + L_q \cdot di_q/dt + \pi v/\tau \cdot \psi_f \end{cases} \quad (4)$$

Substituting (4) into (3) is obtained as:

$$\dot{v}(t) = -B/M v(t) + K_f/M i_q(t) - F_l/M \quad (5)$$

Then the motion equation of the  $i^{\text{th}}$  mover in the multi-movers PMLSM can be described as:

$$\dot{v}_i(t) = \tilde{B}v_i(t) + \tilde{K}i_{q(i)}(t) + \tilde{\lambda}F_{l(i)} \quad (6)$$

where,

$$\begin{cases} \tilde{\lambda} = -1/M < 0 \\ \tilde{B} = -B\tilde{\lambda} > 0 \\ \tilde{K} = K_f\tilde{\lambda} < 0 \end{cases} \quad (7)$$

Considering the uncertainties such as parameter deviation from the nominal value, external load, and unmodeled errors, the motion equation of the PMLSM mover can be described as:

$$\begin{aligned} \dot{v}_i(t) &= (\bar{B}_i + \Delta B_i)v_i(t) + (\bar{K}_i + \Delta K_i)i_{q(i)}(t) \\ &\quad + \tilde{\lambda}F_{l(i)} + \sigma_i \end{aligned} \quad (8)$$

$$= \bar{B}_i v_i(t) + \bar{K}_i i_{q(i)}(t) + D_i(t)$$

$$D_i(t) = \Delta B_i v_i(t) + \Delta K_i i_{q(i)}(t) + \lambda_i F_{l(i)} + \sigma_i \quad (9)$$

where  $\Delta B$  and  $\Delta K$  are the parameter mismatch errors.  $\sigma$  is the unmodeled error.  $D$  is the lumped disturbance, satisfying  $\sup|D| \leq \delta$ .

### B. Ring Coupling Control Strategy

For a PMLSM with  $n$  movers, the block diagram of its ring coupling control strategy is shown in Fig. 1

The error between the actual speed and the command speed is defined as the speed tracking error of the  $i^{\text{th}}$  mover.

$$e_{tr,i}(t) = v_i(t) - v_{cmd}^*(t) \quad (10)$$

Among them,  $e_{tr(i)}$  is the speed tracking error.  $v_{cmd}^*$  is the command speed of all movers.  $v$  is the actual speed of the mover.

The error between the  $i^{\text{th}}$  mover and the  $(i+1)^{\text{th}}$  mover is defined as the synchronization error of the  $i^{\text{th}}$  mover.

$$e_{sync(i)}(t) = v_i(t) - v_{i+1}(t) \quad (11)$$

Thus, the speed controller in Fig. 1 can be designed as shown in Fig. 2.

Among them, the speed controller contains two sub-controllers. One is the speed tracking controller, which is used to accurately track the speed command so that the tracking error can quickly converge to 0. The other is the speed synchronization controller, which is used to synchronize the moving speed of the  $i^{\text{th}}$  mover and the  $(i+1)^{\text{th}}$  mover so that the synchronization error can quickly converge to 0. Therefore, for an  $n$  mover PMLSM,  $2n$  speed controllers need to be designed.

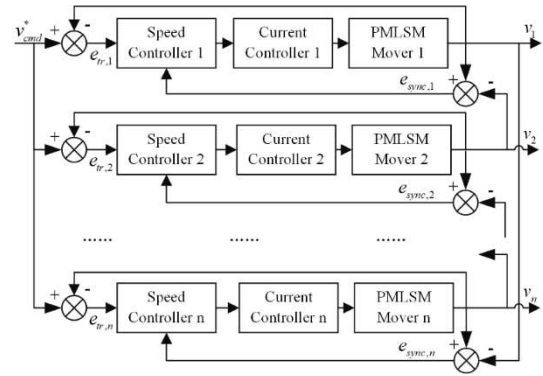


Fig. 1. Ring-coupling control strategy structure

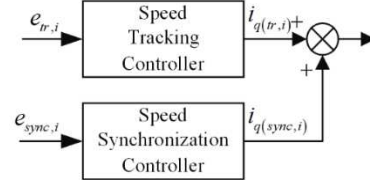


Fig. 2. Speed controller structure

### C. Speed Controller Design

#### 1. Speed Tracking Controller

Combining (8) and (10), the differential form of speed tracking error is described as:

$$\begin{aligned} \dot{e}_{tr(i)}(t) &= \dot{v}_i(t) - \dot{v}_{cmd}^*(t) \\ &= \bar{B}_i v_i(t) + \bar{K}_i i_{q(i)}(t) + D_i(t) - \dot{v}_{cmd}^*(t) \end{aligned} \quad (12)$$

Therefore, to ensure that the speed tracking error converges to 0, the sliding surface  $S_{tr}$  can be designed as:

$$S_{tr(i)}(t) = \alpha e_{tr(i)}(t) + \beta \int_0^t \dot{e}_{tr(i)}(t) dt \quad (13)$$

where  $\alpha > 0$ , and  $\beta > 0$ .

Substituting (12) into (13), the derivative of the sliding surface  $S_{tr}$  can be obtained as:

$$\begin{aligned} \dot{S}_{tr(i)}(t) &= \alpha \dot{e}_{tr(i)}(t) + \beta e_{tr(i)}(t) \\ &= \alpha \left[ \begin{array}{l} \bar{B}_i v_i(t) + \bar{K}_i i_{q(i)}(t) \\ + D_i(t) - \dot{v}_{cmd}^*(t) \end{array} \right] + \beta e_{tr(i)}(t) \end{aligned} \quad (14)$$

The control performance of the speed tracking controller can be obtained by solving the equation  $\dot{S}_{tr(i)}(t) = 0$ . To simplify the calculation process, the (14) is divided into two parts. One part is the nominal model without the lumped error term. The other part is the fitted model under system disturbance.

Under the condition of ignoring the system lumped error ( $D_i(t) = 0$ ), the output result of the controller in the nominal system model can be obtained as:

$$i_{nom(tr,i)}(t) = -(\alpha \bar{K}_i)^{-1} \left[ \beta e_{tr(i)} + \alpha \bar{B}_i v_i(t) - \alpha \dot{v}_{cmd}^* \right] \quad (15)$$

By adding the fitting rate to the sliding surface  $S_{tr(i)}(t)$ , the system can obtain better controller performance under the condition of uncertainty ( $D_i(t) \neq 0$ ). The control output of the fitting part is:

$$i_{fit(tr,i)}(t) = -(\bar{K}_i)^{-1} \mu_{tr(i)} \text{sgn} \left[ S_{tr(i)}(t) \right] \quad (16)$$

Among them,  $\mu_{tr(i)}$  is the switching gain.  $\text{sgn}(\cdot)$  is a sign function.

Combining (15) and (16), the output result of the speed tracking controller of the  $i^{\text{th}}$  mover is:

$$\begin{aligned} i_{q(ir,i)}(t) &= i_{nom(ir,i)}(t) + i_{fit(ir,i)}(t) \\ &= -(\alpha\bar{K}_i)^{-1} \left[ \beta e_{ir(i)} + \alpha\bar{B}_i v_i(t) - \alpha\dot{v}_{cmd}^* \right] \\ &\quad - (\bar{K}_i)^{-1} \mu_{ir(i)} \operatorname{sgn} \left[ S_{ir(i)}(t) \right] \end{aligned} \quad (17)$$

Substituting (17) into (14)  $\dot{S}_{ir}$  can be rewritten as:

$$\begin{aligned} \dot{S}_{ir(i)}(t) &= \alpha \left[ \bar{B}_i v_i(t) + \bar{K}_i i_{q(i)}(t) \right] + \beta e_{ir(i)}(t) \\ &\quad + D_i(t) - \dot{v}_{cmd}^*(t) \\ &= \alpha \left[ \bar{B}_i v_i(t) - \alpha^{-1} \left[ \beta e_{ir(i)} + \alpha\bar{B}_i v_i(t) - \alpha\dot{v}_{cmd}^* \right] \right] \\ &\quad - \mu_{ir(i)} \operatorname{sgn} \left[ S_{ir(i)}(t) \right] + D_i(t) - \dot{v}_{cmd}^* \\ &\quad + \beta e_{ir(i)}(t) \\ &= -\alpha \mu_{ir(i)} \operatorname{sgn} \left[ S_{ir(i)}(t) \right] + \alpha D_i(t) \end{aligned} \quad (18)$$

## 2. Speed Synchronization Controller

Combining (8) and (11), it can be obtained that the differential form of speed synchronization error is:

$$\begin{aligned} \dot{e}_{sync(i)}(t) &= \dot{v}_i(t) - \dot{v}_{i+1}(t) \\ &= \bar{B}_i v_i(t) + \bar{K}_i i_{q(i)}(t) + D_i(t) \\ &\quad - \left[ \bar{B}_{i+1} v_{i+1}(t) + \bar{K}_{i+1} i_{q(i+1)}(t) + D_{i+1}(t) \right] \end{aligned} \quad (19)$$

Therefore, to ensure that the speed synchronization error converges to 0, the sliding surface  $S_{sync(i)}$  can be designed as:

$$S_{sync(i)}(t) = \alpha e_{sync(i)}(t) + \beta \int_0^t e_{sync(i)}(\tau) d\tau \quad (20)$$

Substituting (19) into (20), the first derivative of the sliding surface  $\dot{S}_{sync(i)}$  can be obtained as:

$$\begin{aligned} \dot{S}_{sync(i)}(t) &= \alpha \dot{e}_{sync(i)}(t) + \beta e_{sync(i)}(t) \\ &= \alpha \left[ \bar{B}_i v_i(t) + \bar{K}_i i_{q(i)}(t) + D_i(t) \right] \\ &\quad - \alpha \left[ \bar{B}_{i+1} v_{i+1}(t) + \bar{K}_{i+1} i_{q(i+1)}(t) + D_{i+1}(t) \right] \\ &\quad + \beta e_{sync(i)}(t) \end{aligned} \quad (21)$$

Since both  $\bar{B}$  and  $\bar{K}$  are nominal parameters without considering parameter errors and system disturbances, the following equations hold:

$$\begin{aligned} \bar{B}_i &= \bar{B}_{i+1} = \bar{B}_0 \\ \bar{K}_i &= \bar{K}_{i+1} = \bar{K}_0 \end{aligned} \quad (22)$$

Therefore, (20) can be rewritten as:

$$\begin{aligned} \dot{S}_{sync(i)}(t) &= \alpha \left[ \bar{B}_0 e_{sync(i)}(t) + \bar{K}_0 \begin{pmatrix} i_{q(i)}(t) \\ -i_{q(i+1)}(t) \end{pmatrix} \right] + \beta e_{sync(i)}(t) \\ &\quad + D_i(t) - D_{i+1}(t) \\ &= (\alpha\bar{B}_0 + \beta) e_{sync(i)}(t) + \alpha\bar{K}_0 \Delta i_{q(i)}(t) \\ &\quad + \alpha [D_i(t) - D_{i+1}(t)] \end{aligned} \quad (23)$$

Similarly, under the condition of ignoring the system lumped error ( $D_i(t) = D_{i+1}(t) = 0$ ), the output result of the controller in the nominal system model can be obtained as:

$$i_{nom(sync,i)}(t) = -(\alpha\bar{K}_0)^{-1} (\alpha\bar{B}_0 + \beta) e_{sync(i)}(t) \quad (24)$$

The control output of the fitted part is:

$$i_{fit(sync,i)}(t) = -(\bar{K}_0)^{-1} \mu_{sync(i)} \operatorname{sgn} \left[ S_{sync(i)}(t) \right] \quad (25)$$

Combining (24) and (25), the output result of the speed synchronous controller of the  $i^{\text{th}}$  mover is:

$$\begin{aligned} i_{q(sync,i)}(t) &= i_{nom(sync,i)}(t) + i_{fit(sync,i)}(t) \\ &= -(\alpha\bar{K}_0)^{-1} (\alpha\bar{B}_0 + \beta) e_{sync(i)}(t) \\ &\quad - (\bar{K}_0)^{-1} \mu_{sync(i)} \operatorname{sgn} \left[ S_{sync(i)}(t) \right] \end{aligned} \quad (26)$$

Substituting (26) into (23)  $\dot{S}_{sync}$  can be rewritten as:

$$\begin{aligned} \dot{S}_{sync(i)}(t) &= (\alpha\bar{B}_0 + \beta) e_{sync(i)}(t) + \alpha\bar{K}_0 i_{q(sync,i)}(t) \\ &\quad + \alpha [D_i(t) - D_{i+1}(t)] \\ &= -\alpha \mu_{sync(i)} \operatorname{sgn} \left[ S_{sync(i)}(t) \right] + \alpha [D_i(t) - D_{i+1}(t)] \end{aligned} \quad (27)$$

## 3. Stability Analysis

Theorem 1: The tracking error and synchronization error and their derivative will converge to zero in finite time if the switching gain  $\mu_{ir}$  and  $\mu_{sync}$  are designed as:

$$\begin{cases} \mu_{ref} \geq \delta \\ \mu_{sync} \geq 2\delta \end{cases} \quad (28)$$

*Proof:* The Lyapunov function  $V$  is considered as:

$$V(t) = 0.5 S_{ir(i)}^2(t) + 0.5 S_{sync(i)}^2(t) \quad (29)$$

Then the derivative of the Lyapunov function is:

$$\begin{aligned} \dot{V}(t) &= S_{ir(i)}(t) \dot{S}_{ir(i)}(t) + S_{sync(i)}(t) \dot{S}_{sync(i)}(t) \\ &= \alpha S_{ir(i)}(t) \left[ -\mu_{ir(i)} \operatorname{sgn} \left( S_{ir(i)}(t) \right) + D_i(t) \right] \\ &\quad + \alpha S_{sync(i)}(t) \left[ -\mu_{sync(i)} \operatorname{sgn} \left( S_{sync(i)}(t) \right) \right] \\ &\leq \alpha \left| S_{ir(i)}(t) \right| \left[ \left| D_i(t) \right| - \mu_{ir(i)} \right] \\ &\quad + \alpha \left| S_{sync(i)}(t) \right| \left[ \left| D_i(t) \right| + \left| D_{i+1}(t) \right| - \mu_{sync(i)} \right] \\ &\leq \alpha \left| S_{ir(i)}(t) \right| \left[ \delta - \mu_{ir(i)} \right] \\ &\quad + \alpha \left| S_{sync(i)}(t) \right| \left[ 2\delta - \mu_{sync(i)} \right] \\ &\leq 0 \end{aligned} \quad (30)$$

Therefore, the sliding mode reachable condition is satisfied. This completes the proof of Theorem 1.

## D. Experiment and Analysis

To verify the effectiveness of the proposed method, experiments are carried out on the PMLSM with a four-mover.

Fig. 3 exhibits the established experimental platform. The controller used is the Zmotion ZMC406. And the driver is self-developed by the laboratory. The motor parameters are shown in TABLE I. The parameters used by the controller are shown in TABLE II.

Given that the speed of the four movers is 1m/s and increasing to 1.5m/s at  $t=0.12s$ .

It can be seen from Figure 4 and Figure 5 that when the mover is running stably, the tracking error and synchronization error of the two different control methods are close to zero. When the speed is changed, the proposed method has a smaller

overshoot and higher error accuracy than the relative coupling control. The comparison of the maximum and average error is shown in TABLE III.

TABLE I  
PARAMETERS OF PMLSM

Parameters	$R_s(\Omega)$	$L_d(H)$	$L_q(H)$	$M(Kg)$	Pitch(mm)	$P$	$F_c(N/A)$	$V_{max}(m/s)$
Value	7	0.0265	0.0265	1.1	20	2	37.194	2.5

TABLE II  
PARAMETERS OF THE CONTROLLER

Parameters	Value	Parameters	Value	Parameters	Value
$\alpha$	0.04	$\beta$	235	$\delta$	0.1
$K_p$	200	$K_i$	12		
$\mu_{sync(i)}(i=1,\dots,4)$	295	$\mu_{tr(i)}(i=1,\dots,4)$	365		

TABLE III  
PERFORMANCE COMPARISON BETWEEN RELATIVE COUPLING AND SMC+RING COUPLING

Errors	Method		
	Relative Coupling	SMC+Ring Coupling	
Maximum Error (mm/s)	$e_{tr(1)}$	100.437	35.223
	$e_{tr(2)}$	123.734	37.198
	$e_{tr(3)}$	107.686	42.794
	$e_{tr(4)}$	119.157	41.559
	$e_{sync(1)}$	37.608	13.476
	$e_{sync(2)}$	78.052	7.978
	$e_{sync(3)}$	43.285	7.970
	$e_{sync(4)}$	26.643	7.995
Average Error (mm/s)	$e_{tr(1)}$	-2.820	-0.943
	$e_{tr(2)}$	-0.465	-0.711
	$e_{tr(3)}$	-2.392	-0.701
	$e_{tr(4)}$	-2.337	-0.587
	$e_{sync(1)}$	-1.2871	-0.081
	$e_{sync(2)}$	-0.3545	-0.112
	$e_{sync(3)}$	0.823	-0.133
	$e_{sync(4)}$	-0.431	-0.150

The experimental results show that the tracking performance and synchronization performance of the proposed method is better than the cross-coupling control in the case of disturbances in the control system.

### E. Conclusion

In this article, a ring coupling synchronous control strategy combined with sliding mode control is proposed. This method can guarantee the asymptotic convergence of speed tracking error and synchronization error. The stability is proved by the Lyapunov stability theory. The control scheme is successfully applied in the four-mover PMLSM synchronous control system, and the effectiveness of the proposed synchronous control scheme is verified through experimental analysis and comparison.

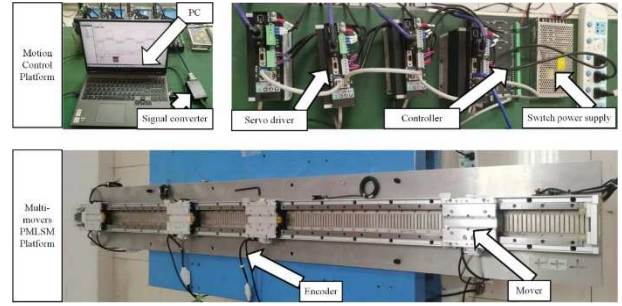


Fig. 3 Four movers PMLSM experiment platform

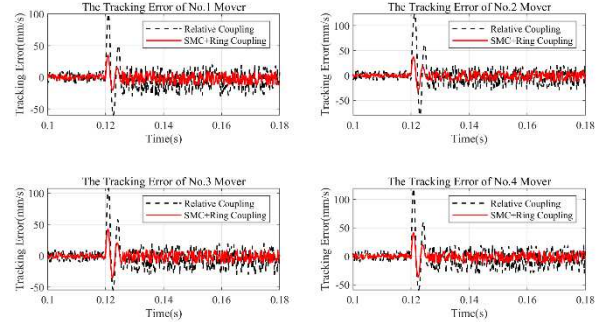


Fig. 4 Comparison of speed tracking error between cross-coupling and SMC+ring coupling

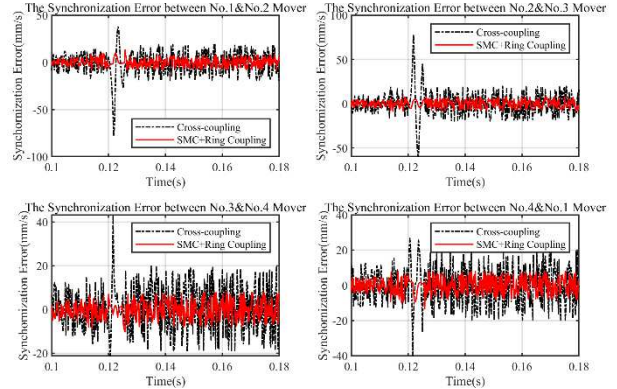


Fig. 5 Comparison of speed synchronization error between cross-coupling and SMC+ring coupling

### ACKNOWLEDGMENT

The work was supported by the National Key R&D Program of China (2020YFB1711300), Major Science and Technology Projects of Guangdong Province, China (2020B090927001), Dongguan Innovation Team Project, China (201536002100026), Guangdong Zhujiang Talent Innovation Team Project, China(2017ZT07G493), Guangdong Basic and Applied Basic Research Foundation(2022A1515110880).

### REFERENCES

- [1] W. X. Zhao, J. Q. Zheng, J. B. Wang, G. H. Liu, J. X. Zhao, and Z. Y. Fang, "Design and Analysis of a Linear Permanent-Magnet Vernier Machine With Improved Force Density," *IEEE Trans. Ind. Electron.*, vol. 63, no. 4, pp. 2072-2082, Apr 2016.
- [2] F. J. Lin, J. C. Hwang, P. H. Chou, and Y. C. Hung, "FPGA-Based Intelligent-Complementary Sliding-Mode Control for PMLSM Servo-Drive System," *IEEE Trans. Power Electron.*, vol. 25, no. 10, pp. 2573-2587, Oct 2010.
- [3] R. W. Cao, Y. Jin, M. H. Lu, and Z. Zhang, "Quantitative Comparison of Linear Flux-Switching Permanent Magnet Motor With Linear Induction

- Motor for Electromagnetic Launch System," *IEEE Trans. Ind. Electron.*, vol. 65, no. 9, pp. 7569-7578, Sep 2018.
- [4] W. T. Su and C. M. Liaw, "Adaptive positioning control for a LPMSM drive based on adapted inverse model and robust disturbance observer," *IEEE Trans. Power Electron.*, vol. 21, no. 2, pp. 505-517, Mar 2006.
- [5] W. Zhao, P. Zhao, D. Xu, Z. Chen, and J. Zhu, "Hybrid modulation fault-tolerant control of open-end windings linear vernier permanent-magnet motor with floating capacitor inverter," *IEEE Trans. Power Electron.*, vol. 34, no. 3, pp. 2563-2572, 2018.
- [6] Z. A. Kuang, H. J. Gao and M. Tomizuka, "Precise Linear-Motor Synchronization Control via Cross-Coupled Second-Order Discrete-Time Fractional-Order Sliding Mode," *IEEE-Asme Transactions on Mechatronics*, vol. 26, no. 1, pp. 358-368, Feb 2021.
- [7] Z. L. Huang, G. Q. Song, Y. M. Li, and M. N. Sun, "Synchronous control of two counter-rotating eccentric rotors in nonlinear coupling vibration system," *Mech. Syst. Sig. Process.*, vol. 114, pp. 68-83, Jan 1, 2019.
- [8] C. Li, C. Li, Z. Chen, and B. Yao, "Advanced Synchronization Control of a Dual-Linear-Motor-Driven Gantry With Rotational Dynamics," *IEEE Trans. Ind. Electron.*, vol. 65, no. 9, pp. 7526-7535, Sep 2018.
- [9] X. J. Yang, H. Liu, D. Lu, and W. H. Zhao, "Investigation of the dynamic electromechanical coupling due to the thrust harmonics in the linear motor feed system," *Mech. Syst. Sig. Process.*, vol. 111, pp. 492-508, Oct 2018.
- [10] L. J. Wang, J. W. Zhao, and Z. L. Zheng, "Robust Speed Tracking Control of Permanent Magnet Synchronous Linear Motor Based on a Discrete-Time Sliding Mode Load Thrust Observer," *IEEE Trans. Ind. Appl.*, vol. 58, no. 4, pp. 4758-4767, Jul-Aug 2022.
- [11] P. W. Shi, W. C. Sun, X. B. Yang, I. J. Rudas, and H. J. Gao, "Master-Slave Synchronous Control of Dual-Drive Gantry Stage With Cogging Force Compensation," *IEEE Transactions on Systems Man Cybernetics-Systems*, vol. 53, no. 1, pp. 216-225, Jan 2023.
- [12] X. Wu, Y. Wu, C. Zhang, and A. Cheng, "A novel synchronous control strategy of combining virtual shaft and deviation coupling," in *2020 7th International Forum on Electrical Engineering and Automation (IFEEA)*, 2020: IEEE, pp. 601-606.
- [13] G. J. Yang, W. R. Wang, J. H. Yan, P. F. Zhi, H. L. Ge, and Z. Y. Zhu, "Improved Multi-Motor Synchronization Control of Underwater Robot Based on Virtual Shaft," *Proceedings of the 33rd Chinese Control and Decision Conference (Ccdc 2021)*, pp. 4652-4657, 2021.
- [14] F. J. Perez-Pinal, C. Nunez, R. Alvarez, and I. Cervantes, "Comparison of Multi-motor Synchronization Techniques," *Iecon 2004: 30th Annual Conference of Ieee Industrial Electronics Society, Vol 2*, pp. 1670-1675, 2004.
- [15] Y. Koren, "Cross-coupled biaxial computer control for manufacturing systems," 1980.
- [16] J. Li, Y. T. Fang, X. Y. Huang, and J. Li, "Comparison of Synchronization Control Techniques for Traction Motors of High-Speed Trains," *2014 17th International Conference on Electrical Machines and Systems (Icems)*, pp. 2114-2119, 2014.
- [17] D. Sun, "Position synchronization of multiple motion axes with adaptive coupling control," *Automatica*, vol. 39, no. 6, pp. 997-1005, 2003.
- [18] F. J. Perez-Pinal, G. Calderon and I. Araujo-Vargas, "Relative coupling strategy," in *IEEE International Electric Machines and Drives Conference, 2003. IEMDC'03.*, 2003, vol. 2: IEEE, pp. 1162-1166.
- [19] J. Z. Sun, R. Liu, Y. Q. Luo, and W. Sun, "Research on Multi-motor Synchronization Control for Cutter Head of Shield Machine Based on the Ring Coupled Control Strategy," *Intelligent Robotics and Applications, Proceedings*, vol. 5928, pp. 345+, 2009.
- [20] R. Liu, J. Z. Sun, Y. Q. Luo, W. Sun, and W. D. Li, "Research on Multi-motor Synchronization Control Based on the Ring Coupling Strategy for Cutterhead Driving System of Shield Machines," *Advances in Mechanical Engineering, Pts 1-3*, vol. 52-54, pp. 65+, 2011.